

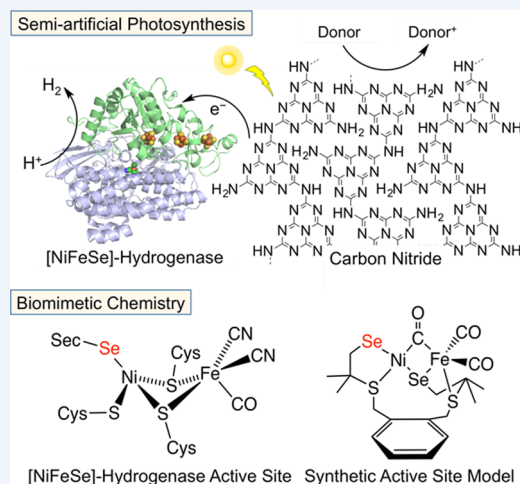
# [NiFeSe]-Hydrogenase Chemistry

Claire Wombwell,<sup>‡</sup> Christine A. Caputo,<sup>‡</sup> and Erwin Reisner\*

Christian Doppler Laboratory for Sustainable SynGas Chemistry, Department of Chemistry, University of Cambridge, Lensfield Road, Cambridge CB2 1EW, U.K.

**CONSPECTUS:** The development of technology for the inexpensive generation of the renewable energy vector H<sub>2</sub> through water splitting is of immediate economic, ecological, and humanitarian interest. Recent interest in hydrogenases has been fueled by their exceptionally high catalytic rates for H<sub>2</sub> production at a marginal overpotential, which is presently only matched by the non-scalable noble metal platinum. The mechanistic understanding of hydrogenase function guides the design of synthetic catalysts, and selection of a suitable hydrogenase enables direct applications in electro- and photocatalysis. [FeFe]-hydrogenases display excellent H<sub>2</sub> evolution activity, but they are irreversibly damaged upon exposure to O<sub>2</sub>, which currently prevents their use in full water splitting systems. O<sub>2</sub>-tolerant [NiFe]-hydrogenases are known, but they are typically strongly biased toward H<sub>2</sub> oxidation, while H<sub>2</sub> production by [NiFe]-hydrogenases is often product (H<sub>2</sub>) inhibited. [NiFeSe]-hydrogenases are a subclass of [NiFe]-hydrogenases with a selenocysteine residue coordinated to the active site nickel center in place of a cysteine. They exhibit a combination of unique properties that are highly advantageous for applications in water splitting compared with other hydrogenases. They display a high H<sub>2</sub> evolution rate with marginal inhibition by H<sub>2</sub> and tolerance to O<sub>2</sub>. [NiFeSe]-hydrogenases are therefore one of the most active molecular H<sub>2</sub> evolution catalysts applicable in water splitting. Herein, we summarize our recent progress in exploring the unique chemistry of [NiFeSe]-hydrogenases through biomimetic model chemistry and the chemistry with [NiFeSe]-hydrogenases in semiartificial photosynthetic systems. We gain perspective from the structural, spectroscopic, and electrochemical properties of the [NiFeSe]-hydrogenases and compare them with the chemistry of synthetic models of this hydrogenase active site. Our synthetic models give insight into the effects on the electronic properties and reactivity of the active site upon the introduction of selenium.

We have utilized the exceptional properties of the [NiFeSe]-hydrogenase from *Desulfomicrobium baculatum* in a number of photocatalytic H<sub>2</sub> production schemes, which are benchmark systems in terms of single site activity, tolerance toward O<sub>2</sub>, and *in vitro* water splitting with biological molecules. Each system comprises a light-harvesting component, which allows for light-driven electron transfer to the hydrogenase in order for it to catalyze H<sub>2</sub> production. A system with [NiFeSe]-hydrogenase on a dye-sensitized TiO<sub>2</sub> nanoparticle gives an enzyme–semiconductor hybrid for visible light-driven generation of H<sub>2</sub> with an enzyme-based turnover frequency of 50 s<sup>-1</sup>. A stable and inexpensive polymeric carbon nitride as a photosensitizer in combination with the [NiFeSe]-hydrogenase shows good activity for more than 2 days. Light-driven H<sub>2</sub> evolution with the enzyme and an organic dye under high O<sub>2</sub> levels demonstrates the excellent robustness and feasibility of water splitting with a hydrogenase-based scheme. This has led, most recently, to the development of a light-driven full water splitting system with a [NiFeSe]-hydrogenase wired to the water oxidation enzyme photosystem II in a photoelectrochemical cell. In contrast to the other systems, this photoelectrochemical system does not rely on a sacrificial electron donor and allowed us to establish the long sought after light-driven water splitting with an isolated hydrogenase.



## 1. INTRODUCTION

Enormous effort is currently invested in the establishment of natural and artificial photosynthetic systems for efficient, sunlight-driven water splitting into the renewable fuel H<sub>2</sub> and byproduct O<sub>2</sub>. The development of H<sub>2</sub> evolution catalysts is central to this effort. Nature has evolved extremely efficient enzymes called hydrogenases, to reversibly catalyze the interconversion of protons and electrons with H<sub>2</sub>.<sup>1</sup> Hydrogenases operate with remarkably high turnover frequencies of up to 10<sup>4</sup> s<sup>-1</sup> at a small overpotential and are therefore the most efficient noble-metal-free H<sub>2</sub> production catalysts.<sup>2</sup> This activity

is achieved at an active site containing either two iron centers in [FeFe]-hydrogenases or one iron and one nickel center in [NiFe]-hydrogenases. The metal center of the hydrogenase active site contains a primary coordination sphere with cysteine, 2-azapropanedithiolate (only in [FeFe]-hydrogenases), carbon monoxide, and cyanide ligands. Thus, hydrogenases serve as a benchmark, and as a blueprint to inspire the design of synthetic 3d transition metal catalysts.

Received: July 10, 2015

Published: October 21, 2015

In this Account, we summarize our work on [NiFeSe]-hydrogenase; a selenium-containing subclass of the [NiFe]-hydrogenase. Selenium is present in proteins in the amino acid selenocysteine (Sec).<sup>3</sup> The incorporation of selenocysteine into a protein comes with a high energetic cost to an organism due to the specific translation machineries required for selenocysteine synthesis.<sup>4</sup> Therefore, there must be a specific function of selenocysteine that is not exhibited by the sulfur-containing analogue, cysteine. The [NiFeSe]-hydrogenase is an intriguing example of nature's use of selenium, and its active site is identical to that of the [NiFe]-hydrogenases except for the replacement of a terminally coordinated cysteine residue by selenocysteine (Figure 1).<sup>5</sup>

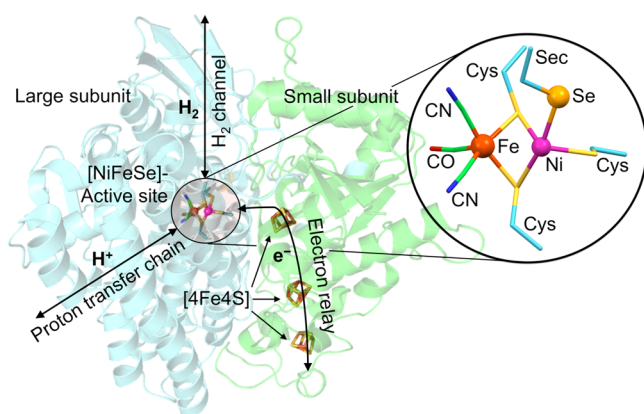


**Figure 1.** Ribbon representation of the [NiFeSe]-hydrogenase from *Desulfomicrobium baculatum* with schematic indication of movement of substrates and products between the enzyme surface and the enzyme active site.<sup>6</sup>

We explore the unique chemistry of [NiFeSe]-hydrogenases through biomimetic chemistry to gain insight into the role of selenium in the active site, and exploit the excellent activity of the enzyme for solar fuel synthesis in semiautomatic photosynthetic systems. The synthesis, spectroscopic and structural features, as well as reactivity, of model complexes of the [NiFeSe]-hydrogenase active site will be highlighted. Several photocatalytic systems and a light-driven water splitting cell with [NiFeSe]-hydrogenase that makes use of the exceptional activity of this enzyme will also be discussed.

## 2. UNIQUE PROPERTIES OF THE [NiFeSe]-HYDROGENASES

[NiFeSe]-hydrogenases exhibit a number of advantageous properties for H<sub>2</sub> production systems. First, the selenium-containing hydrogenases generally display high H<sub>2</sub> production activity compared with [NiFe]-hydrogenases, which makes them good candidates as H<sub>2</sub> evolution biocatalysts.<sup>7–11</sup> The high activity of this subclass is explained by a stronger kinetic bias toward H<sub>2</sub> production,<sup>5,7,8,10,12</sup> and a lack of substantial inhibition of H<sub>2</sub> production by H<sub>2</sub> product compared with the [NiFe]-hydrogenases.<sup>2,8,9,11,12</sup> A protein film voltammogram of the *Desulfomicrobium baculatum* [NiFeSe]-hydrogenase on an indium tin oxide (ITO) electrode with a hierarchical morphology is given in Figure 2A.<sup>13</sup> The voltammograms show the potential dependent catalytic currents for H<sub>2</sub> oxidation and production with a narrow cut through zero current indicating thermodynamic reversibility. Finally, the [NiFeSe]-hydrogenase also displays fast reactivation from O<sub>2</sub>

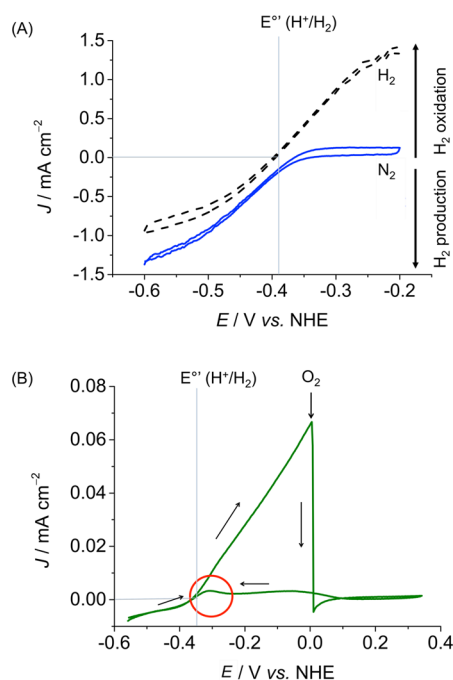


**Figure 2.** (A) Protein film voltammogram of a stationary nanostructured ITO electrode with adsorbed *Desulfomicrobium baculatum* [NiFeSe]-hydrogenase in a pH 6.5 electrolyte solution with stirring showing both H<sub>2</sub> production and oxidation under an atmosphere of 100% N<sub>2</sub> (solid trace) and 100% H<sub>2</sub> (1 bar, dashed trace).<sup>13</sup> (B) Voltammogram recorded at 1 mV s<sup>-1</sup> (arrows denoting the scan direction) with the same enzyme adsorbed on a pyrolytic graphite edge rotating disc electrode showing H<sub>2</sub> oxidation (under 100% H<sub>2</sub>) with injection of O<sub>2</sub> saturated buffer (pH 6) at 0 V vs. NHE followed by removal of O<sub>2</sub> by flushing the headspace with H<sub>2</sub>. The rapid reactivation process can be observed during the reverse scan (circled).<sup>8</sup>

inactivation at a low redox potential indicative of O<sub>2</sub> tolerance.<sup>8,14</sup> This effect is demonstrated in Figure 2B, where reactivation of the enzyme was observed at cathodic potentials following injection of an O<sub>2</sub> saturated electrolyte solution and purging of the headspace with H<sub>2</sub>.<sup>8</sup> The O<sub>2</sub> sensitivity of *Desulfomicrobium baculatum* [NiFeSe]-hydrogenase during H<sub>2</sub> oxidation at positive potentials prevents its use in enzyme fuel cells and other applications, and we therefore focus only on its unique H<sub>2</sub> evolution activity.<sup>2,8</sup>

A direct comparison of the distinct activity was reported for the [NiFeSe]- and [NiFe]-hydrogenase from *Desulfovibrio vulgaris* Hildenborough. Inclusion of selenium in the growth medium of this bacterium leads to expression of [NiFeSe]-hydrogenase with suppressed levels of [FeFe]- and [NiFe]-hydrogenases being produced. [NiFeSe]-hydrogenase cannot be isolated in the absence of selenium, and to compensate, more of the other hydrogenases are expressed. The activity of the [NiFeSe]-hydrogenase for H<sub>2</sub> production was reported to be 40 times higher than the corresponding [NiFe]-hydrogenase.<sup>7</sup>

### 2.1. Chemical Basis for High Activity

The nickel ion serves as the active redox center in the [NiFeSe]- and [NiFe]-hydrogenases: its oxidation state varies between nickel(I), nickel(II), and nickel(III), whereas a low-spin iron(II) is present in all states. The [NiFe]-hydrogenase has been characterized in three distinct catalytically active states, namely Ni-SI<sub>o</sub>, Ni-R, and Ni-C.<sup>1,15–17</sup> By analogy, characteristic Ni-C signals are also exhibited in the infrared and

electron paramagnetic resonance spectrum of a number of [NiFeSe]-hydrogenases and the Ni-R state has been observed for the [NiFeSe]-hydrogenase from *Desulfovibrio vulgaris* Hildenborough as the most reduced state (Figure 3).<sup>7,11,14,16,17</sup> Although the [NiFeSe]-hydrogenase has not

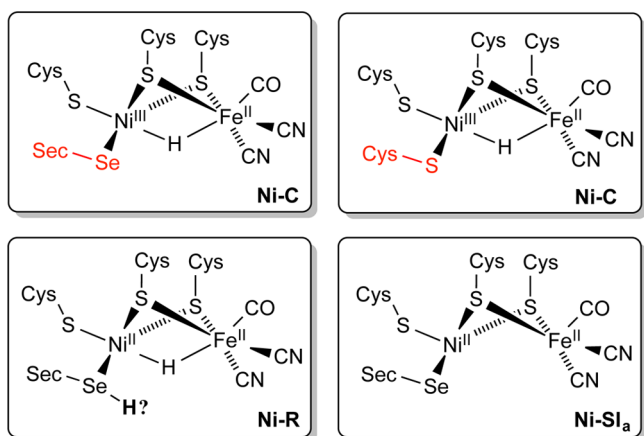


**Figure 3.** Active site structure of [NiFeSe]- and [NiFe]-hydrogenases in the catalytically active Ni-C state<sup>18</sup> and proposed Ni-R and Ni-SI<sub>a</sub> states for the [NiFeSe]-hydrogenases.<sup>15</sup>

been characterized in the Ni-SI<sub>a</sub> state, the mechanisms of the two hydrogenases are likely to follow a similar pathway, and thus a Ni-SI<sub>a</sub> like state is proposed to also exist for the [NiFeSe]-hydrogenases.

In the [NiFe]-hydrogenases, the cysteine thiolate highlighted in Figure 3 has been proposed to act as a proton relay during H<sub>2</sub> cycling because this cysteine residue is present in a number of different positions in the crystal structure, indicating conformational flexibility arising from various protonation states of the thiolate.<sup>19</sup> The selenocysteine also has a high temperature factor in the crystal structure of the [NiFeSe]-hydrogenase, indicating that the selenolate may be protonated.<sup>6,19</sup> It has thus been proposed that protons are delivered via an intraprotein proton transfer chain to selenocysteine to protonate the hydride in the heterobimetallic center to form H<sub>2</sub>.<sup>3,5,20</sup> A nucleophilic addition mechanism was suggested for heterolytic cleavage of H<sub>2</sub> in [NiFe]-hydrogenases, and the higher nucleophilicity of selenocysteine than cysteine may therefore be relevant for the higher activity of the selenium containing subclass.<sup>3,21–23</sup> The pK<sub>a</sub> of a selenocysteine selenol at 5.2 is lower than the pK<sub>a</sub> of a cysteine thiol at 8.0, which would also facilitate protonation of the hydride to form H<sub>2</sub>.<sup>3</sup> However, these mechanistic considerations are still speculative because the direct detection of protons in the hydrogenase active site remains a challenge. The possibility of protonation at a metal center, needs to be investigated further through biochemical analysis and biomimetic chemistry.

The overall protein structure is almost identical among different [NiFeSe]- and [NiFe]-hydrogenase types and is made up of a minimum of two subunits.<sup>6,18,19,24–27</sup> Figure 1 gives a schematic representation of the movement of substrates and products to and from the active site. The active site is buried deep within the large subunit. The small subunit generally contains three iron–sulfur clusters, which make up an electron transfer chain that enables electron transport between the active site and the enzyme surface. They are assigned as the proximal,

medial, and distal clusters, based on their distance from the active site. In the standard (O<sub>2</sub>-sensitive) [NiFe]-hydrogenases, the proximal and distal clusters are [4Fe4S], whereas the medial cluster is [3Fe4S].<sup>1,18,19,24</sup> An exception are the O<sub>2</sub>-tolerant, membrane-bound [NiFe]-hydrogenases, which contain a proximal [4Fe3S] cluster and were suggested to perform two sequential one-electron transfers to reduce O<sub>2</sub> at the active site.<sup>28</sup> In [NiFeSe]-hydrogenases, however, all three clusters have a [4Fe4S] composition.<sup>6,19,25–27</sup> These differences may be critical in tuning the electronic properties of these enzymes.

H<sub>2</sub> is proposed to move between the hydrogenase active site and enzyme surface through a hydrophobic channel.<sup>29,30</sup> Molecular dynamics simulations performed on the *Desulfomicrobium baculatum* [NiFeSe]-hydrogenase revealed that the partition coefficient of H<sub>2</sub> between the active site and the surrounding water is much higher than in *Desulfovibrio gigas* [NiFe]-hydrogenase. The [NiFeSe]-hydrogenase possesses an additional H<sub>2</sub> diffusion pathway and can accommodate a higher concentration of H<sub>2</sub> close to the active site.<sup>31,32</sup> These differences are likely to have an impact on enzymatic activity and H<sub>2</sub> inhibition.

## 2.2. Fast Reactivation from Oxidative Damage and O<sub>2</sub>-Tolerance

Both the [NiFe]- and [NiFeSe]-hydrogenases are reversibly inactivated by O<sub>2</sub> or anaerobic oxidation and require reactivation through reduction, either by exposure to H<sub>2</sub> or by the application of a negative electrochemical potential.<sup>8,11,14,20,33–35</sup> The key difference between the enzymes is an extremely rapid reactivation for the [NiFeSe]-hydrogenase, whereas anaerobic reactivation of the standard [NiFe]-hydrogenase is a slow process that can take several hours.<sup>7,8,12,20,33,34,36</sup>

The standard [NiFe]-hydrogenase exists in two aerobically isolated states, known as Ni-A (unready) and Ni-B (ready), in varying ratios. Incubation of the hydrogenase for several hours under a H<sub>2</sub>-containing, O<sub>2</sub>-free atmosphere is required to reactivate the Ni-A state, whereas Ni-B can be reactivated within seconds. These inactive states are reformed upon reoxidation either chemically (O<sub>2</sub> exposure) or electrochemically (anodic potential).<sup>20,33,34</sup> When the standard [NiFe]-hydrogenase is isolated aerobically, the nickel center is oxidized to nickel(III) to form the Ni-A and Ni-B states. There is a bridging ligand between the two metal centers in both of these inactive states.<sup>20,24,33,34,37</sup> There are “nonstandard” [NiFe]-hydrogenases that exhibit aerobic H<sub>2</sub> oxidation, namely, the O<sub>2</sub>-tolerant, membrane-bound [NiFe]-hydrogenase from *Ralstonia eutropha*, the soluble O<sub>2</sub>-tolerant hydrogenases, and the regulatory hydrogenases.<sup>28</sup>

Protein film electrochemistry of the *Desulfomicrobium baculatum* [NiFeSe]-hydrogenase showed that anaerobic inactivation of this enzyme does not occur at positive potentials provided that the concentration of H<sub>2</sub> is above a certain level.<sup>8</sup> In the presence of O<sub>2</sub>, two inactive states form, which can be distinguished by the potentials at which they reactivate. One state is preferentially formed under a H<sub>2</sub> containing atmosphere and is reactivated at the same potential as the anaerobically inactivated hydrogenase. The other aerobically inactivated state reactivates very rapidly at potentials close to that of the H<sup>+</sup>/H<sub>2</sub> reduction potential (Figure 2B).<sup>8</sup>

In contrast to the standard [NiFe]-hydrogenase, a nickel(III) state has not been detected for the oxidized [NiFeSe]-hydrogenase, additional bridging ligands between the nickel

and iron centers are not observed, and the selenocysteine selenium and, in some cases, a cysteine sulfur is oxidized in the oxidized and as isolated states.<sup>7,11,16,36,38–40</sup> Oxidation of a nickel-coordinated cysteine sulfur has also been reported in the crystal structure of an oxidized [NiFe]-hydrogenase.<sup>37</sup> The X-ray crystal structures of the oxidized [NiFeSe]-hydrogenases from *Desulfovibrio vulgaris* Hildenborough,<sup>25,27</sup> and *Desulfomicrobium baculatum*<sup>26</sup> have been reported, and the structural composition of the oxidized active sites are shown in Figure 4.

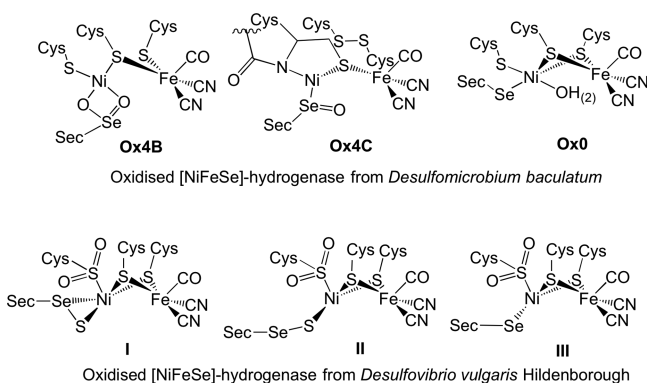


**Figure 4.** Oxidized active site structures of the *Desulfomicrobium baculatum* [NiFeSe]-hydrogenase<sup>26</sup> and the *Desulfovibrio vulgaris* Hildenborough [NiFeSe]-hydrogenase (different structures with partial occupancy shown).<sup>25,27</sup>

The anaerobically purified *Desulfomicrobium baculatum* [NiFeSe]-hydrogenase was crystallized aerobically. Three main active site structures were solved with various selenium oxidation states and different ligands at nickel: Ox4B, Ox4C, and Ox0.<sup>26</sup> Similarly, in the *Desulfovibrio vulgaris* Hildenborough [NiFeSe]-hydrogenase, which was both purified and crystallized aerobically, the active site exists in three states with partial occupancy. In two of these states, selenium is oxidized.<sup>25,27</sup>

The oxidation of selenium in selenocysteine is more facile than that of sulfur in cysteine. Oxidation of the selenium in several structures of the [NiFeSe]-hydrogenase suggests that it may protect nickel from oxidative attack.<sup>41,42</sup> In addition, oxidized selenium is more easily reduced than oxidized sulfur,<sup>43</sup> and selenium–oxygen bonds are weaker than the corresponding sulfur–oxygen bonds.<sup>43–45</sup> The increased size of the

selenium atom compared with sulfur also makes the active site more sterically congested.<sup>25</sup> The addition of selenium may therefore sterically block and chemically protect the nickel center from O<sub>2</sub> attack. The oxidized selenium species is more easily reduced in accord with the fast reactivation of the [NiFeSe]-hydrogenases from O<sub>2</sub> inactivation and the full recovery of H<sub>2</sub> production activity after inactivation following O<sub>2</sub> removal from the cell.<sup>8</sup> Thus, the more bulky selenium and the ease with which selenocysteine is oxidized and reduced back to the active form could explain the increased O<sub>2</sub>-tolerance of [NiFeSe]-hydrogenases.

### 3. SYNTHETIC ACTIVE SITE MODELS

The first structural active site models of the [NiFeSe]-hydrogenases have been reported.<sup>46,47</sup> First, a series of four complexes with the general composition [Ni(L<sup>E</sup>)(Mes<sup>E</sup>)]<sup>−</sup>, where L<sup>E</sup> = 2,2'-thiodibenzenethiol (E' = S) or 2-((2-hydroxyphenyl)thio)benzenethiol (E' = Se) and Mes<sup>E</sup> = mesityl thiolate (E = S) or mesityl selenolate (E = Se), were synthesized to emulate the primary coordination sphere of the nickel site of the [NiFeSe]-hydrogenases (Figure 5).<sup>46</sup> The selenium and sulfur containing compounds are isostructural and exhibit square planar geometry around the nickel center. However, the Ni–SeMes distances (2.306(3) Å) are longer than the Ni–SMes distances (2.189(3) Å). A Ni–Se bond length of 2.46 Å and average Ni–S distance of 2.2 Å was reported for the reduced [NiFeSe]-hydrogenase from *Desulfomicrobium baculatum* (2.15 Å resolution).<sup>6</sup>

The reactivity of complexes [Ni(L<sup>S</sup>)(Mes<sup>Se</sup>)]<sup>−</sup> and [Ni(L<sup>S</sup>)(Mes<sup>S</sup>)]<sup>−</sup> with O<sub>2</sub> was investigated by exposing a solution of the complexes to atmospheric O<sub>2</sub>. Upon oxidation of [Ni(L<sup>S</sup>)(Mes<sup>Se</sup>)]<sup>−</sup>, dimesityl diselenide was formed, which was accompanied by the loss of the ligand from the nickel center (Figure 5B). Oxidation of selenium, the formation of a selenium–chalcogen bond, and concomitant loss of selenium from the metal center are all features observed in the oxidized *Desulfovibrio vulgaris* Hildenborough [NiFeSe]-hydrogenase (Figure 4).<sup>25,27</sup> The selenolate containing complex [Ni(L<sup>S</sup>)(Mes<sup>Se</sup>)]<sup>−</sup> was oxidized four times more rapidly than the corresponding all thiolate complex [Ni(L<sup>S</sup>)(Mes<sup>S</sup>)]<sup>−</sup>, which supports the hypothesis that fast oxidation of selenium may prevent the nickel center from being oxidized.<sup>25–27</sup> Exposure of [Ni(L<sup>S</sup>)(Mes<sup>Se</sup>)]<sup>−</sup> to 1 equiv of HBF<sub>4</sub> resulted in protonation and loss of Mes<sup>Se</sup> as mesityl selenol from the metal center

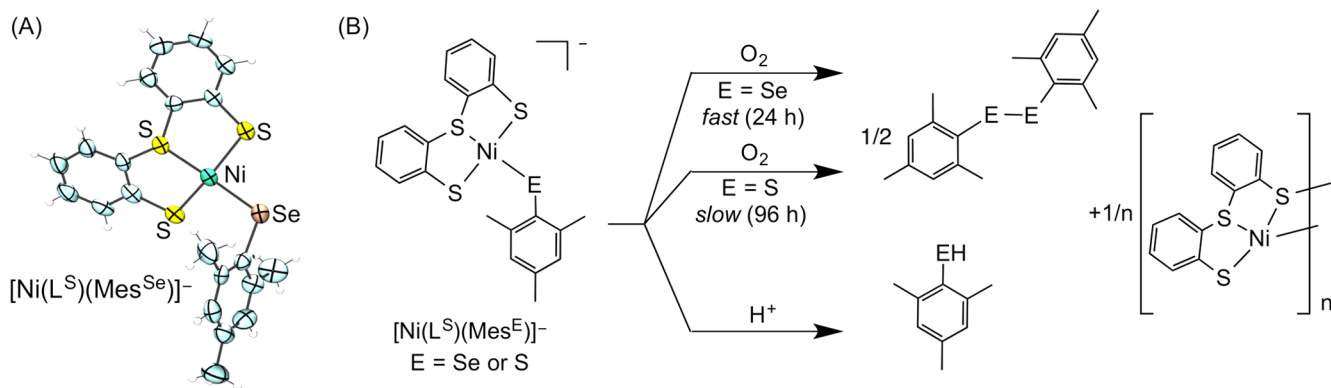


**Figure 5.** (A) X-ray single crystal structure of the nickel subsite model complex (n-Bu<sub>4</sub>N)[Ni(L<sup>S</sup>)(Mes<sup>Se</sup>)] showing 50% probability ellipsoids (gray = carbon, white = hydrogen, counteraction not shown). (B) Structure and reactivity of the active site model complexes [Ni(L<sup>S</sup>)(Mes<sup>Se</sup>)]<sup>−</sup> and [Ni(L<sup>S</sup>)(Mes<sup>S</sup>)]<sup>−</sup> with O<sub>2</sub> (top) and HBF<sub>4</sub> (bottom).<sup>46</sup>

(Figure 5B), demonstrating that the selenolate can be protonated by a strong acid.

The only dinuclear [NiFeSe]-hydrogenase active site model reported to date is [NiFe("S<sub>2</sub>Se<sub>2</sub>")(CO)<sub>3</sub>], which features a doubly bridged heterobimetallic nickel and iron center with a selenolate terminally coordinated to the nickel center and carbonyl ligands at the iron (Figure 6).<sup>47</sup> The complex is

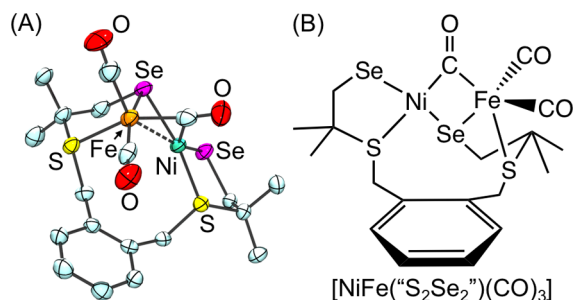


**Figure 6.** (A) X-ray single crystal structure of the model complex [NiFe("S<sub>2</sub>Se<sub>2</sub>")(CO)<sub>3</sub>] showing 50% probability ellipsoids (gray = carbon, hydrogen atoms omitted for clarity) and (B) chemical structure.<sup>47</sup>

structurally analogous to the [NiFe]-hydrogenase model [NiFe("S<sub>4</sub>")(CO)<sub>3</sub>], where selenium is replaced by sulfur.<sup>48</sup> The Ni–Se(terminal) distance in [NiFe("S<sub>2</sub>Se<sub>2</sub>")(CO)<sub>3</sub>] is 2.28 Å, compared with a Ni–S(terminal) distance of 2.16 Å in [NiFe("S<sub>4</sub>")(CO)<sub>3</sub>].<sup>48</sup> The introduction of selenium does not significantly affect any of the other distances in the model complexes: the Ni–Fe distance is only marginally longer (0.02 Å) in [NiFe("S<sub>2</sub>Se<sub>2</sub>")(CO)<sub>3</sub>], and the distances between the metal and the bridging carbonyl carbon are almost identical.

All three CO stretching frequencies in the infrared spectrum of [NiFe("S<sub>2</sub>Se<sub>2</sub>")(CO)<sub>3</sub>] (2000, 1942, and 1835 cm<sup>-1</sup>) are lower than those for [NiFe("S<sub>4</sub>")(CO)<sub>3</sub>] (2003, 1943, and 1842 cm<sup>-1</sup>),<sup>48</sup> indicating increased d-to-π\* back-donation due to increased electron density at the metal centers. The absorption bands exhibited by [NiFe("S<sub>2</sub>Se<sub>2</sub>")(CO)<sub>3</sub>] are all red-shifted relative to [NiFe("S<sub>4</sub>")(CO)<sub>3</sub>] as expected, due to the increased size and polarizability of selenium relative to sulfur. An increase in electron density at the bimetallic core could also lower its reduction potential and might also contribute to the stronger bias toward H<sub>2</sub> production in the selenium-containing enzyme.

These [NiFeSe]-active site model complexes do not display electrocatalytic activity as homogeneous H<sub>2</sub> production catalysts. The complexes are not sufficiently active or stable at a cathodic potential in the presence of a proton source. However, the model complexes act as molecular precursors to form nickel and/or iron containing solid-state deposits, which are active as heterogeneous H<sub>2</sub> production catalysts in pH neutral water.<sup>46,47</sup>

#### 4. PHOTOCATALYTIC H<sub>2</sub> PRODUCTION SYSTEMS

The elucidation of the unique features of the [NiFeSe]-hydrogenases for electrocatalytic H<sub>2</sub> production<sup>8</sup> has enabled the rapid development of semiartificial photocatalytic H<sub>2</sub> production systems with this enzyme from *Desulfomicrobium baculatum*.<sup>9,49,50</sup> We have established that this hydrogenase can be rationally combined with a range of light harvesting materials, in either homogeneous or heterogeneous systems, and thereby acts as a versatile and highly active electrocatalyst in photochemical schemes (Figure 7).

The first use of this hydrogenase for photocatalytic H<sub>2</sub> production was demonstrated by the attachment of the enzyme to a ruthenium dye-sensitized TiO<sub>2</sub> nanoparticle (Figure 7B).<sup>9,51</sup> The ruthenium dye (RuP) was attached to the TiO<sub>2</sub> particle via phosphonic acid linkers. Immobilization of the enzyme close to the distal iron–sulfur cluster, [4Fe4S]<sub>dist</sub>, is essential for electronic communication and electron flow into the active site. *Desulfomicrobium baculatum* [NiFeSe]-hydrogenase has a large number of surface-exposed glutamate and aspartate residues in close proximity to [4Fe4S]<sub>dist</sub>, which may act as natural anchor sites, via the carboxylate, to the metal oxide surface. These provided strong interfacial interactions that allowed for an almost quantitative binding of the enzyme to the TiO<sub>2</sub> surface, although not all bound enzyme was necessarily functional.<sup>9,52</sup> This system operates by visible light excitation of the ruthenium dye, which is followed by electron injection into the TiO<sub>2</sub> conduction band. Subsequent electron transfer from the conduction band to the [NiFeSe]-hydrogenase allows for catalytic H<sub>2</sub> production with a turnover frequency up to 50 mol of H<sub>2</sub> (mol of hydrogenase)<sup>-1</sup> s<sup>-1</sup> in the presence of a sacrificial electron donor. Photo-H<sub>2</sub> production was monitored for up to 8 h, giving a TON up to 1.9 × 10<sup>5</sup>, but the photostability of the ruthenium dye led to cessation of the activity upon further irradiation.<sup>51</sup>

*Desulfomicrobium baculatum* [NiFeSe]-hydrogenase significantly outperforms a range of other hydrogenases on dye-

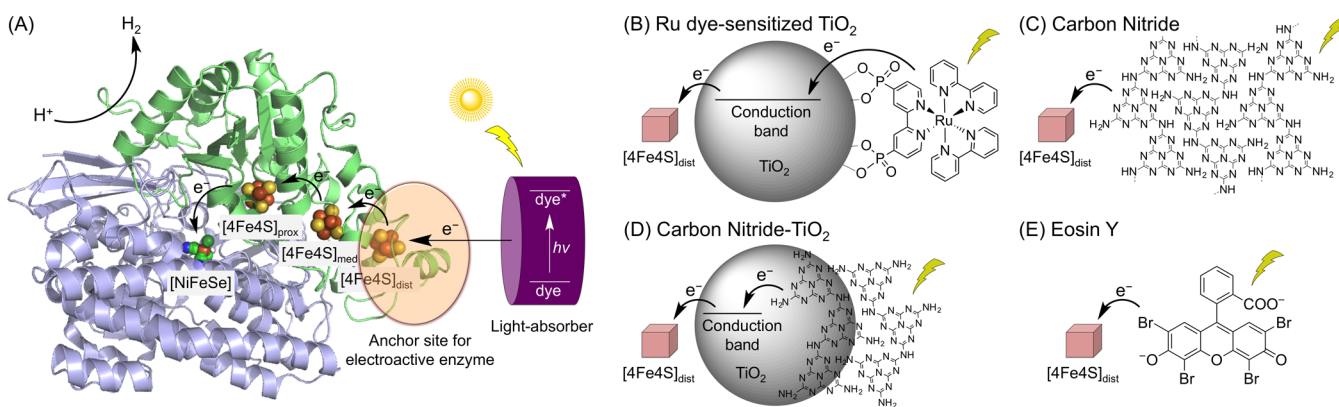


**Figure 7.** (A) General representation of hybrid [NiFeSe]-hydrogenase photocatalytic systems for visible light-driven H<sub>2</sub> production using (B) RuP–TiO<sub>2</sub>,<sup>9</sup> (C) CN<sub>x</sub>,<sup>49</sup> (D) CN<sub>x</sub>–TiO<sub>2</sub>,<sup>53</sup> and (E) Eosin Y<sup>50</sup> as photosensitizers in the presence of a sacrificial electron donor.

sensitized TiO<sub>2</sub>, including the H<sub>2</sub>-producing [FeFe]-hydrogenases from *Clostridium acetobutylicum* and *Chlamydomonas reinhardtii*, the O<sub>2</sub>-tolerant, membrane-bound [NiFe]-hydrogenase from *Ralstonia eutropha*, and the O<sub>2</sub>-tolerant and H<sub>2</sub> producing Hyd-2 [NiFe]-hydrogenase from *Escherichia coli* (all of which show more than 80% lower activity).<sup>9</sup> The high H<sub>2</sub> production activity, tolerance toward H<sub>2</sub>, and good O<sub>2</sub> stability of this hydrogenase, as well as its favorable orientation upon attachment to TiO<sub>2</sub>, are believed to be responsible for its superior activity.<sup>9,49–51</sup>

The system was further advanced by replacing the ruthenium dye with a less expensive and more stable light absorber. Amorphous, polymeric CN<sub>x</sub> is a 2D material synthesized by the thermolysis of urea or melamine<sup>54</sup> and was used as a heterogeneous photosensitizer with the [NiFeSe]-hydrogenase to give a system with turnover frequencies of 5532 mol of H<sub>2</sub> (mol of hydrogenase)<sup>-1</sup> h<sup>-1</sup> under solar light irradiation and a sacrificial electron donor (Figure 7C).<sup>49</sup> The use of CN<sub>x</sub> significantly enhanced the stability of the system, which remained active after 2 days, giving a turnover number >50 000 for H<sub>2</sub> production.<sup>49</sup> The weak interaction of the enzyme with CN<sub>x</sub> limited the performance of this system.

Improvements in integrating CN<sub>x</sub> with the [NiFeSe]-hydrogenase were required. Thus, the enzyme was adsorbed onto a hybrid material in which CN<sub>x</sub> was grafted onto the surface of TiO<sub>2</sub> (Figure 7D). This approach allowed nearly quantitative binding of the “titanophilic” hydrogenase and improved electron transfer through the stronger electronic coupling at the material–enzyme interface.<sup>53</sup> The CN<sub>x</sub>-TiO<sub>2</sub> hybrid operates through two distinct mechanistic pathways during visible light irradiation. Photoexcitation of CN<sub>x</sub> results in promotion of an electron into the LUMO of CN<sub>x</sub>, followed by electron transfer into the conduction band of TiO<sub>2</sub>. In addition, the formation of a charge transfer complex occurs, whereby the excited electrons are promoted directly from the HOMO of the CN<sub>x</sub> to the TiO<sub>2</sub> conduction band. This additional pathway extends the light absorption further into the visible region compared with CN<sub>x</sub> alone. This sacrificial system achieved a turnover number of more than 5.8 × 10<sup>5</sup> in 72 h. In the presence of a redox mediator, methyl viologen, a turnover number of up to 3.8 million was observed.

With high activity and stability established in photocatalytic schemes under anaerobic conditions, we demonstrated photo-H<sub>2</sub> production with *Desulfomicrobium baculatum* [NiFeSe]-hydrogenase in a homogeneous system under O<sub>2</sub>.<sup>50</sup> Eosin Y was selected as a dye and was shown to be able to inject electrons directly to the [NiFeSe]-hydrogenase upon excitation without requiring the use of a soluble redox mediator (Figure 7E). The system was found to produce H<sub>2</sub> with a turnover frequency of 13.9 mol of H<sub>2</sub> (mol of hydrogenase)<sup>-1</sup> s<sup>-1</sup> in the presence of a sacrificial electron donor, under inert conditions, and retained 11% activity in the presence of atmospheric levels of O<sub>2</sub>.

The excellent activity of *Desulfomicrobium baculatum* [NiFeSe]-hydrogenase has most recently allowed for the first demonstration of *ex vivo* water splitting into H<sub>2</sub> and O<sub>2</sub> with a hydrogenase. Here, the [NiFeSe]-hydrogenase was immobilized on a hierarchical, inverse opal mesoporous ITO cathode and wired to the water oxidation enzyme photosystem II in a photoelectrochemical cell (Figures 2A and 8).<sup>13</sup> Irradiation of the photosystem II photoanode resulted in the production of H<sub>2</sub> and O<sub>2</sub> in a 2:1 ratio and a 5.4% photon-to-hydrogen energy conversion efficiency under low intensity red light irradiation

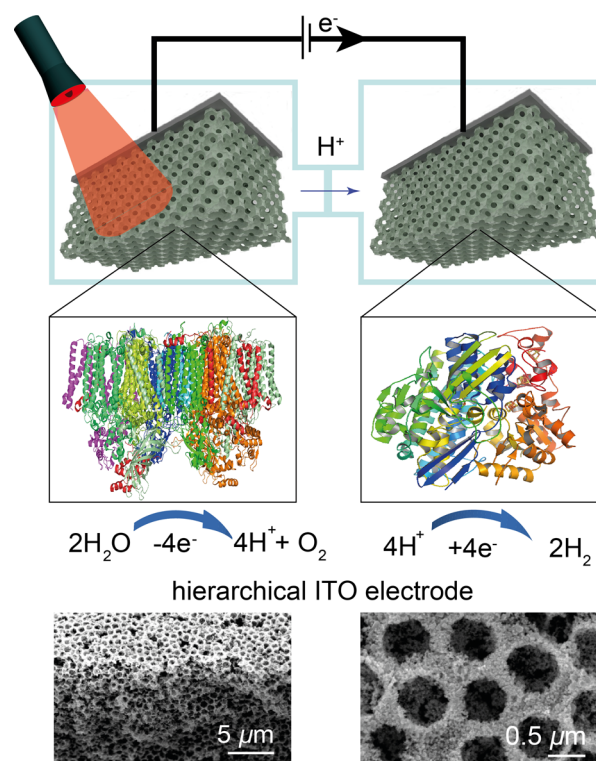


**Figure 8.** Photoelectrochemical cell for complete water splitting with photosystem II wired to [NiFeSe]-hydrogenase. Both enzymes were immobilized on hierarchical ITO, which enabled excellent integration of the enzymes in the artificial circuitry of the cell. Water oxidation occurred at the photosystem II photoanode and electrons were transferred to the [NiFeSe]-hydrogenase via the external circuit.<sup>13</sup>

with an applied bias potential of 0.8 V. This prototype system is the first example of photoelectrochemical solar fuel synthesis with wired enzymes.

## 5. CONCLUSIONS AND PROSPECTS

[NiFeSe]-hydrogenases display a combination of unique properties required for application in water splitting, which are available to a much lesser extent in standard [NiFe]- and [FeFe]-hydrogenases. A prototype example is *Desulfomicrobium baculatum* [NiFeSe]-hydrogenase, which exhibits a bias toward H<sub>2</sub> evolution in the presence of O<sub>2</sub> and displays little product (H<sub>2</sub>) inhibition.<sup>6–8,10</sup> These features combined make this enzyme, arguably, the most efficient molecular H<sub>2</sub> evolution catalyst for use in water splitting. Thus, we are developing [NiFeSe]-hydrogenase chemistry through the mimicry of this enzyme’s active site to understand its unique activity and to employ this enzyme as the electrocatalyst in semiartificial photosynthesis.

Our synthetic models of the [NiFeSe]-hydrogenase active site<sup>46,47</sup> have shown that the introduction of a coordinated selenium ligand can fine-tune the electronic properties of the heterobimetallic core. The increased size and polarizability of selenium relative to sulfur and the related facile oxidation and reduction of selenocysteine relative to cysteine are likely to be contributing factors for the high proton reduction activity, quick oxidation of selenocysteine to protect the transition metal core, and fast reactivation upon O<sub>2</sub>-inactivation in the [NiFeSe]-hydrogenase. Although our biomimetic studies support these properties, the exact role of selenium and the possibility for secondary coordination sphere effects in

improving the performance of this enzyme remain unknown and a conclusive rationale for the use of selenocysteine in the [NiFeSe]-hydrogenases, as well as other selenocysteine containing enzymes, is yet to be discovered.

[NiFeSe]-hydrogenase from *Desulfomicrobium baculatum* can now be rationally combined with light absorbing materials such as dye-sensitized metal oxide semiconductors, carbon nitrides, and homogeneous photosensitizers such as Eosin Y.<sup>9,49,50</sup> The resulting systems display excellent photocatalytic activities with stabilities up to a couple of days and turnover numbers above one million.<sup>53</sup> They thus easily outperform purely synthetic systems containing noble- and toxic-metal-free electrocatalysts based on single-site catalytic performance. Further improvements will rely on improving the enzyme–light absorber interface to better control the orientation and binding of the enzyme. Although this enzyme is fragile and requires careful handling, we also demonstrate that this enzyme can be added to complex functional systems, much like a chemical reagent. A milestone in hydrogenase-based H<sub>2</sub> production was recently reached with the assembly of a light-driven full water splitting cell with [NiFeSe]-hydrogenase wired to photosystem II.<sup>13</sup> This demonstrates that sacrificial agents can be avoided in light-driven H<sub>2</sub> production and opens exciting opportunities for using this enzyme to catalyze the endergonic reactions required for solar fuel synthesis. This photoelectrochemical system is limited by the fragility of photosystem II, and future challenges are the assembly of more robust water splitting systems and the incorporation of [NiFeSe]-hydrogenase into photosynthetic *in vivo* systems.

## AUTHOR INFORMATION

### Corresponding Author

\*E-mail: [reisner@ch.cam.ac.uk](mailto:reisner@ch.cam.ac.uk). Website: <http://www-reisner.ch.cam.ac.uk/>.

### Author Contributions

‡C.W. and C.A.C. contributed equally to this work

### Notes

The authors declare no competing financial interest.

### Biographies

**Claire Wombwell** studied Chemistry at The University of Sheffield and obtained her Ph.D. from the University of Cambridge in 2014. Her research has focused on bioinorganic chemistry and electrocatalytic hydrogen production.

**Christine A. Caputo** received her Ph.D. from Western Ontario in 2009. She held Postdoctoral Research Fellowships at the University of California Davis and at Cambridge University and is now an Assistant Professor at the University of New Hampshire. Her research interests include synthetic main group chemistry and the use of earth abundant complexes for sustainable solar fuel generation.

**Erwin Reisner** is a University Reader and director of the Christian Doppler Laboratory in the Department of Chemistry of the University of Cambridge. His interests lie in chemical biology, synthetic chemistry, materials science, and engineering relevant to the development of artificial photosynthesis.

## ACKNOWLEDGMENTS

We acknowledge support by the Christian Doppler Research Association (Austrian Federal Ministry of Science, Research and Economy and National Foundation for Research,

Technology and Development), the OMV Group, the EPSRC (Grant EP/H00338X/2 to E.R.), and a Marie Curie fellowship (Grant GAN 624997 to C.C.). We also thank Mr. David Wakerley and Dr. Bertrand Reuillard for helpful comments and Dr. Juan C. Fontecilla-Camps and his group for providing us with *Desulfomicrobium baculatum* [NiFeSe]-hydrogenase over the years.

## REFERENCES

- (1) Lubitz, W.; Ogata, H.; Rüdiger, O.; Reijerse, E. Hydrogenases. *Chem. Rev.* **2014**, *114*, 4081–4148.
- (2) Vincent, K. A.; Parkin, A.; Armstrong, F. A. Investigating and exploiting the electrocatalytic properties of hydrogenases. *Chem. Rev.* **2007**, *107*, 4366–4413.
- (3) Arnér, E. S. J. Selenoproteins—What unique properties can arise with selenocysteine in place of cysteine? *Exp. Cell Res.* **2010**, *316*, 1296–1303.
- (4) Yoshizawa, S.; Böck, A. The many levels of control on bacterial selenoprotein synthesis. *Biochim. Biophys. Acta, Gen. Subj.* **2009**, *1790*, 1404–1414.
- (5) Baltazar, C. S. A.; Marques, M. C.; Soares, C. M.; DeLacey, A. M.; Pereira, I. A. C.; Matias, P. M. Nickel–Iron–Selenium Hydrogenases – An Overview. *Eur. J. Inorg. Chem.* **2011**, 948–962.
- (6) Garcin, E.; Vernede, X.; Hatchikian, E. C.; Volbeda, A.; Frey, M.; Fontecilla-Camps, J. C. The crystal structure of a reduced [NiFeSe] hydrogenase provides an image of the activated catalytic center. *Structure* **1999**, *7*, 557–566.
- (7) Valente, F. M. A.; Oliveira, A. S. F.; Gnadet, N.; Pacheco, I.; Coelho, A. V.; Xavier, A. V.; Teixeira, M.; Soares, C. M.; Pereira, I. A. C. Hydrogenases in *Desulfovibrio vulgaris* Hildenborough: structural and physiologic characterisation of the membrane-bound [NiFeSe] hydrogenase. *J. Biol. Inorg. Chem.* **2005**, *10*, 667–682.
- (8) Parkin, A.; Goldet, G.; Cavazza, C.; Fontecilla-Camps, J. C.; Armstrong, F. A. The difference a Se makes? Oxygen-tolerant hydrogen production by the [NiFeSe]-hydrogenase from *Desulfomicrobium baculatum*. *J. Am. Chem. Soc.* **2008**, *130*, 13410–13416.
- (9) Reisner, E.; Powell, D. J.; Cavazza, C.; Fontecilla-Camps, J. C.; Armstrong, F. A. Visible light-driven H<sub>2</sub> production by hydrogenases attached to dye-sensitized TiO<sub>2</sub> nanoparticles. *J. Am. Chem. Soc.* **2009**, *131*, 18457–18466.
- (10) Valente, F. M. A.; Almeida, C. C.; Pacheco, I.; Carita, J.; Saraiva, L. M.; Pereira, I. A. C. Selenium is involved in regulation of periplasmic hydrogenase gene expression in *Desulfovibrio vulgaris* Hildenborough. *J. Bacteriol.* **2006**, *188*, 3228–3235.
- (11) Riethausen, J.; Rüdiger, O.; Gärtner, W.; Lubitz, W.; Shafaat, H. S. Spectroscopic and electrochemical characterization of the [NiFeSe] hydrogenase from *Desulfovibrio vulgaris* Miyazaki F: Reversible redox behavior and interactions between electron transfer centers. *ChemBioChem* **2013**, *14*, 1714–1719.
- (12) Gutiérrez-Sánchez, C.; Rüdiger, O.; Fernández, V. M.; De Lacey, A. L.; Marques, M.; Pereira, I. A. C. Interaction of the active site of the Ni–Fe–Se hydrogenase from *Desulfovibrio vulgaris* Hildenborough with carbon monoxide and oxygen inhibitors. *J. Biol. Inorg. Chem.* **2010**, *15*, 1285–1292.
- (13) Mersch, D.; Lee, C.-Y.; Zhang, J. Z.; Brinkert, K.; Fontecilla-Camps, J. C.; Rutherford, A. W.; Reisner, E. Wiring of photosystem II to hydrogenase for photoelectrochemical water-splitting. *J. Am. Chem. Soc.* **2015**, *137*, 8541–8549.
- (14) De Lacey, A. L.; Gutiérrez-Sánchez, C.; Fernández, V. M.; Pacheco, I.; Pereira, I. A. C. FTIR spectroelectrochemical characterization of the Ni–Fe–Se hydrogenase from *Desulfovibrio vulgaris* Hildenborough. *J. Biol. Inorg. Chem.* **2008**, *13*, 1315–1320.
- (15) Krämer, T.; Kampa, M.; Lubitz, W.; van Gestel, M.; Neese, F. Theoretical spectroscopy of the Ni<sup>II</sup> intermediate states in the catalytic cycle and the activation of [NiFe] hydrogenases. *ChemBioChem* **2013**, *14*, 1898–1905.
- (16) Medina, M.; Hatchikian, E. C.; Cammack, R. Studies of light-induced nickel EPR signals in hydrogenase: comparison of enzymes

with and without selenium. *Biochim. Biophys. Acta, Bioenerg.* **1996**, *1275*, 227–236.

(17) Stein, M.; Lubitz, W. The electronic structure of the catalytic intermediate Ni-C in [NiFe] and [NiFeSe] hydrogenases. *Phys. Chem. Chem. Phys.* **2001**, *3*, 5115–5120.

(18) Volbeda, A.; Charon, M.-H.; Piras, C.; Hatchikian, E. C.; Frey, M.; Fontecilla-Camps, J. C. Crystal structure of the nickel–iron hydrogenase from *Desulfovibrio gigas*. *Nature* **1995**, *373*, 580–587.

(19) Fontecilla-Camps, J. C.; Volbeda, A.; Cavazza, C.; Nicolet, Y. Structure/function relationships of [NiFe]- and [FeFe]-hydrogenases. *Chem. Rev.* **2007**, *107*, 4273–4303.

(20) De Lacey, A. L.; Fernández, V. M.; Rousset, M.; Cammack, R. Activation and inactivation of hydrogenase function and the catalytic cycle: Spectroelectrochemical studies. *Chem. Rev.* **2007**, *107*, 4304–4330.

(21) Niu, S.; Hall, M. B. Modeling the Active Sites in Metalloenzymes 5. The heterolytic bond cleavage of H<sub>2</sub> in the [NiFe] hydrogenase of *Desulfovibrio gigas* by a Nucleophilic Addition Mechanism. *Inorg. Chem.* **2001**, *40*, 6201–6203.

(22) Huber, R. E.; Criddle, R. S. Comparison of the chemical properties of selenocysteine and selenocystine with their sulfur analogs. *Arch. Biochem. Biophys.* **1967**, *122*, 164–173.

(23) Pleasants, J. C.; Guo, W.; Rabenstein, D. L. A comparative study of the kinetics of selenol/diselenide and thiol/disulfide exchange reactions. *J. Am. Chem. Soc.* **1989**, *111*, 6553–6558.

(24) Ogata, H.; Kellers, P.; Lubitz, W. The crystal structure of the [NiFe] hydrogenase from the photosynthetic bacterium *Allochroa vinosum*: Characterization of the oxidized enzyme (Ni-A state). *J. Mol. Biol.* **2010**, *402*, 428–444.

(25) Marques, M. C.; Coelho, R.; De Lacey, A. L.; Pereira, I. A. C.; Matias, P. M. The three-dimensional structure of [NiFeSe] hydrogenase from *Desulfovibrio vulgaris* Hildenborough: A hydrogenase without a bridging ligand in the active site in its oxidised, “as-isolated” state. *J. Mol. Biol.* **2010**, *396*, 893–907.

(26) Volbeda, A.; Amara, P.; Iannello, M.; De Lacey, A. L.; Cavazza, C.; Fontecilla-Camps, J. C. Structural foundations for the O<sub>2</sub> resistance of *Desulfomicrobium baculatum* [NiFeSe]-hydrogenase. *Chem. Commun.* **2013**, *49*, 7061–7063.

(27) Marques, M. C.; Coelho, R.; Pereira, I. A. C.; Matias, P. M. Redox state-dependent changes in the crystal structure of [NiFeSe] hydrogenase from *Desulfovibrio vulgaris* Hildenborough. *Int. J. Hydrogen Energy* **2013**, *38*, 8664–8682.

(28) Shafaat, H. S.; Rüdiger, O.; Ogata, H.; Lubitz, W. [NiFe] hydrogenases: a common active site for hydrogen metabolism under diverse conditions. *Biochim. Biophys. Acta, Bioenerg.* **2013**, *1827*, 986–1002.

(29) Fontecilla-Camps, J. C.; Amara, P.; Cavazza, C.; Nicolet, Y.; Volbeda, A. Structure–function relationships of anaerobic gas-processing metalloenzymes. *Nature* **2009**, *460*, 814–822.

(30) Montet, Y.; Amara, P.; Volbeda, A.; Verne, X.; Hatchikian, E. C.; Field, M. J.; Frey, M.; Fontecilla-Camps, J. C. Gas access to the active site of Ni-Fe hydrogenases probed by X-ray crystallography and molecular dynamics. *Nat. Struct. Biol.* **1997**, *4*, 523–526.

(31) Baltazar, C. S. A.; Teixeira, V. H.; Soares, C. M. Structural features of [NiFeSe] and [NiFe] hydrogenases determining their different properties: a computational approach. *J. Biol. Inorg. Chem.* **2012**, *17*, 543–555.

(32) Gutiérrez-Sanz, O.; Marques, M. C.; Baltazar, C. S. A.; Fernández, V. M.; Soares, C. M.; Pereira, I. A.; De Lacey, A. L. Influence of the protein structure surrounding the active site on the catalytic activity of [NiFeSe] hydrogenases. *J. Biol. Inorg. Chem.* **2013**, *18*, 419–427.

(33) Vincent, K. A.; Parkin, A.; Lenz, O.; Albracht, S. P. J.; Fontecilla-Camps, J. C.; Cammack, R.; Friedrich, B.; Armstrong, F. A. Electrochemical definitions of O<sub>2</sub> sensitivity and oxidative inactivation in hydrogenases. *J. Am. Chem. Soc.* **2005**, *127*, 18179–18189.

(34) Abou Hamdan, A.; Burlat, B.; Gutiérrez-Sanz, O.; Liebgott, P.-P.; Baffert, C.; De Lacey, A. L.; Rousset, M.; Guigliarelli, B.; Léger, C.;

Dementin, S. O<sub>2</sub>-independent formation of the inactive states of NiFe hydrogenase. *Nat. Chem. Biol.* **2013**, *9*, 15–17.

(35) Wakerley, D. W.; Reisner, E. Oxygen-tolerant proton reduction catalysis: much O<sub>2</sub> about nothing? *Energy Environ. Sci.* **2015**, *8*, 2283–2295.

(36) Teixeira, M.; Fauque, G.; Moura, I.; Lespinat, P. A.; Berlier, Y.; Prickril, B.; Peck, H. D.; Xavier, A. V.; Le Gall, J.; Moura, J. J. G. Nickel-[iron-sulfur]-selenium-containing hydrogenases from *Desulfovibrio baculatus* (DSM 1743). *Eur. J. Biochem.* **1987**, *167*, 47–58.

(37) Ogata, H.; Hirota, S.; Nakahara, A.; Komori, H.; Shibata, N.; Kato, T.; Kano, K.; Higuchi, Y. Activation process of [NiFe] hydrogenase elucidated by high-resolution X-ray analyses: Conversion of the ready to the unready state. *Structure* **2005**, *13*, 1635–1642.

(38) Teixeira, M.; Moura, I.; Fauque, G.; Czechowski, M.; Berlier, Y.; Lespinat, P. A.; Le Gall, J.; Xavier, A. V.; Moura, J. J. G. Redox properties and activity studies on a nickel-containing hydrogenase isolated from a halophilic sulfate reducer *Desulfovibrio salaxigens*. *Biochimie* **1986**, *68*, 75–84.

(39) Bingemann, R.; Klein, A. Conversion of the central [4Fe–4S] cluster into a [3Fe–4S] cluster leads to reduced hydrogen-uptake activity of the F<sub>420</sub>-reducing hydrogenase of *Methanococcus voltae*. *Eur. J. Biochem.* **2000**, *267*, 6612–6618.

(40) Rieder, R.; Cammack, R.; Hall, D. O. Purification and properties of the soluble hydrogenase from *Desulfovibrio desulfuricans* (strain Norway 4). *Eur. J. Biochem.* **1984**, *145*, 637–643.

(41) Skaff, O.; Pattison, D. I.; Morgan, P. E.; Bachana, R.; Jain, V. K.; Priyadarini, K. I.; Davies, M. J. Selenium-containing amino acids are targets for myeloperoxidase-derived hypothiocyanous acid: determination of absolute rate constants and implications for biological damage. *Biochem. J.* **2012**, *441*, 305–316.

(42) Cardey, B.; Enescu, M. Selenocysteine versus cysteine reactivity: A theoretical study of their oxidation by hydrogen peroxide. *J. Phys. Chem. A* **2007**, *111*, 673–678.

(43) Hondal, R. J.; Ruggles, E. L. Differing views of the role of selenium in thioredoxin reductase. *Amino Acids* **2011**, *41*, 73–89.

(44) Smoes, S.; Drowart, J. Determination of the dissociation energy of selenium monoxide by the mass-spectrometric Knudsen-cell method. *J. Chem. Soc., Faraday Trans. 2* **1984**, *80*, 1171–1180.

(45) Benson, S. W. Thermochemistry and kinetics of sulfur-containing molecules and radicals. *Chem. Rev.* **1978**, *78*, 23–35.

(46) Wombwell, C.; Reisner, E. Synthesis, structure and reactivity of Ni site models of [NiFeSe] hydrogenases. *Dalton Trans.* **2014**, *43*, 4483–4493.

(47) Wombwell, C.; Reisner, E. Synthetic active site model of the [NiFeSe] hydrogenase. *Chem. - Eur. J.* **2015**, *21*, 8096–8104.

(48) Weber, K.; Krämer, T.; Shafaat, H. S.; Weyhermüller, T.; Bill, E.; van Gestel, M.; Neese, F.; Lubitz, W. A functional [NiFe]-hydrogenase model compound that undergoes biologically relevant reversible thiolate protonation. *J. Am. Chem. Soc.* **2012**, *134*, 20745–20755.

(49) Caputo, C. A.; Gross, M. A.; Lau, V. W.; Cavazza, C.; Lotsch, B. V.; Reisner, E. Photocatalytic hydrogen production using polymeric carbon nitride with a hydrogenase and a bioinspired synthetic Ni catalyst. *Angew. Chem., Int. Ed.* **2014**, *53*, 11538–11542.

(50) Sakai, T.; Mersch, D.; Reisner, E. Photocatalytic hydrogen evolution with a hydrogenase in a mediator-free system under high levels of oxygen. *Angew. Chem., Int. Ed.* **2013**, *52*, 12313–12316.

(51) Reisner, E.; Fontecilla-Camps, J. C.; Armstrong, F. A. Catalytic electrochemistry of a [NiFeSe]-hydrogenase on TiO<sub>2</sub> and demonstration of its suitability for visible-light driven H<sub>2</sub> production. *Chem. Commun.* **2009**, 550–552.

(52) Reisner, E. Solar hydrogen evolution with hydrogenases: From natural to hybrid systems. *Eur. J. Inorg. Chem.* **2011**, 1005–1016.

(53) Caputo, C. A.; Wang, L.; Beranek, R.; Reisner, E. Carbon nitride-TiO<sub>2</sub> hybrid modified with hydrogenase for visible light driven hydrogen production. *Chem. Sci.* **2015**, *6*, 5690–5694.

(54) Wang, X.; Maeda, K.; Thomas, A.; Takahashi, K.; Xin, G.; Carlsson, J. M.; Domen, K.; Antonietti, M. A metal-free polymeric photocatalyst for hydrogen production from water under visible light. *Nat. Mater.* **2009**, *8*, 76–80.